Ultrafast electron dynamics manipulation of laser induced periodic ripples via a train of shaped pulses

2013 Laser Phys. Lett. 10 026003

(http://iopscience.iop.org/1612-202X/10/2/026003)

Laser Phys. Lett. **10** (2013) 026003 (4pp) doi:10.1088/1612-2011/10/2/026003

LETTER

Ultrafast electron dynamics manipulation of laser induced periodic ripples via a train of shaped pulses

G Du, Q Yang, F Chen, H Bian, X Meng, J Si, F Yun and X Hou

State Key Laboratory for Manufacturing System Engineering and Key Laboratory of Photonics Technology for Information of Shaanxi Province, School of Electronics and Information Engineering, Xi'an Jiaotong University, Xi'an 710049, People's Republic of China

E-mail: yangqing@mail.xjtu.edu.cn and chenfeng@mail.xjtu.edu.cn

Received 10 July 2012
Accepted for publication 2 October 2012
Published 7 January 2013
Online at stacks.iop.org/LPL/10/026003

Abstract
We present the electron dynamics manipulation of laser induced periodic nanoripples on fused silica via a train of shaped femtosecond pulses. The non-linear ionization used for supporting the surface plasmon polaritons (SPPs) is taken into account in the analysis of the ripple dynamics. It is revealed that the ripple periods are closely related to both the pulse-to-pulse separation and the laser fluence. The result is attributed to the ultrafast dynamics manipulation for the SPP dispersion wavelength through the unusual ionization arising via a train of shaped pulses. This study should be helpful for the fundamental understanding of the ripple formation mechanism arising from a train of shaped pulses, used for controlling the ripple features.

(Some figures may appear in colour only in the online journal)

1. Introduction

Laser induced periodic surface structures (LIPSSs), or ripples, have been widely studied because of their potential interest in both scientific and practical aspects [1–4]. More recently, trains of temporally shaped femtosecond pulses, namely multi-pulse sequences with various separations, have attracted great attention in the laser patterning field [5–9]. High ablation efficiency and reduced thermal recasting can be achieved by applying a train of shaped pulses.

Recently, surface plasmon polariton (SPP) interference with the wide-spectrum femtosecond pulses was frequently reported as the ripple formation mechanism [10–12]. When a dielectric is irradiated by a train of shaped pulses, the material is initially ionized by the pulse that is ahead, and the pre-ionized region then interacts with the following pulse phase, leading to the formation of absorption enhanced nanoplasma cores. The free electrons supporting the SPPs on the dielectrics can be triggered by the ionization dynamics in the region of the ionized cores. The SPPs can therefore be generated in the ionization zone due to the scattering nanosphere assisted wavevector matching [13]. Itina *et al* revealed that the transient ionization dynamics achieved via a train of shaped pulses can be unprecedentedly adjusted through the correlation of the pulse-to-pulse separation, leading to distinctive electron excitation consequences for material ablation [14]. This indicates that the SPPs supported by the ionization dynamics can be modulated by shaping the pulse configuration. Although the static models ignoring the ionization dynamics, such as those of surface scattering wave interference [15], first-principles theory [16], and second-harmonic interaction [17], can explain many of the general features of ripples, accurate predictions of the ripple modifications via the train of temporally shaped pulses remain a challenge.

In this letter, we theoretically investigate the electron dynamics manipulation in laser induced nanoripple formation on fused silica under irradiation with a train of shaped double

femtosecond (fs) pulses. The non-linear ionization triggered SPPs, the plasma relaxation and the transient interference phase matching for ripple formation with respect to the train of shaped pulses are investigated using a dynamics model. This reveals that the ripple period modifications with respect to the pulse separation and the fluence of the train of shaped pulses can be well predicted by the dynamics model.

2. Theoretical modeling and methods

In the early stage of the formation of ripples on dielectrics via irradiation with temporally shaped femtosecond pulses, the material is initially ionized by the leading pulse phase of the train of shaped pulses via the multi-phonon and avalanche mechanisms. The SPPs are simultaneously generated in the ionized region due to the scattering nanosphere assisted wavevector matching. The following pulse phases of the temporally shaped femtosecond laser will interact with the pre-ionized region (the optical properties modification region). The transient interferences between the SPPs and the wide-spectrum femtosecond pulse are taken as the ripple formation mechanism [10, 11]. The condition for formation of the nanoripples follows the wavevector-matching relationship for interference described by the momentum conservation law written as follows:

$$\vec{k}_{\mathrm{G}} = \vec{k}_{\mathrm{SP}} - \vec{k}_{\mathrm{P}} \tag{1}$$

where $\vec{k}_{\mathrm{P}}$ and $\vec{k}_{\mathrm{SP}}$ are the wavevectors of the incident laser and the excited SPPs, respectively, and $\vec{k}_{\mathrm{G}}$ is the wavevector of the patterned nanoripples, described as $2\pi/\Lambda$ with Λ denoting the ripple period.

The dispersion relationship for the excited SPPs is presented as

$$\lambda_{\mathrm{SP}} = \lambda\,\mathrm{Re}\left[\left(\frac{\varepsilon_1+\varepsilon_2}{\varepsilon_1\varepsilon_2}\right)^{1/2}\right] \tag{2}$$

where λ_{SP} and λ denote the wavelengths for SPPs and the incident laser, and ε_1 and ε_2 are, respectively, the permittivities of the excited dielectric and ambient medium separated by the interface. Also

$$\varepsilon_1 = 1 + (\varepsilon_{\mathrm{g}} - 1)\left(\frac{N_{\mathrm{V}} - N_{\mathrm{e}}}{N_{\mathrm{V}}}\right) - \frac{N_{\mathrm{e}}}{N_{\mathrm{c}}}\frac{1}{1 + \mathrm{i}(\omega\tau_{\mathrm{c}})^{-1}} \tag{3}$$

where ε_{g} is the dielectric function of the nonexcited fused silica, N_{e} is the number density of the ionized electron plasma, N_{V} is the density of the valence electrons, $N_{\mathrm{c}} = \omega^2 m_{\mathrm{e}}\varepsilon_0/e^2$ is the critical electron density, ω is the frequency of the incident laser, and τ_{c} accounts for the collision time written as

$$\tau_{\mathrm{c}} = \left(\frac{M}{m_{\mathrm{e}}}\right)^{1/2}\frac{\hbar}{J_{\mathrm{i}}}\left(\frac{N_{\mathrm{e}}}{N_{\mathrm{c}}}\right)^{1/3} \tag{4}$$

where M is the atomic mass unit, $\hbar$ is the reduced Planck constant, and J_{i} is the ionization energy.

The initial non-linear ionization dynamics for fused silica is presented as

$$\frac{\partial N_{\mathrm{e}}}{\partial t} = \frac{N_{\mathrm{V}} - N_{\mathrm{e}}}{N_{\mathrm{V}}}(\alpha N_{\mathrm{V}} + \beta N_{\mathrm{e}}) + \sigma N_{\mathrm{s}} I^m - \frac{N_{\mathrm{e}}}{\tau_{\mathrm{e}}} \tag{5}$$

$$\frac{\partial N_{\mathrm{s}}}{\partial t} = -\sigma N_{\mathrm{s}} I^m + \frac{N_{\mathrm{e}}}{\tau_{\mathrm{s}}} \tag{6}$$

where: N_{s} is the number density of self-trapped excitons (STEs); I is laser intensity, which decays into the fused silica following the non-linear absorption mechanisms [14]; m is the number of photons needed for STE excitation ($m = 5$); τ_{e} is the lifetime of the electron plasma relaxation due to trapping and recombination, which is in the range from several hundreds of fs to a few ps; σ is the multi-photon cross section for STEs; and τ_{s} is the lifetime of the STEs. α and β, respectively, are the multi-photon and avalanche ionization rates, which can be written as

$$\alpha \approx \omega n_{\mathrm{ph}}^{3/2}\left(\frac{\varepsilon_{\mathrm{osc}}}{2J_{\mathrm{i}}}\right)^{n_{\mathrm{ph}}} \tag{7}$$

$$\beta \approx \frac{\varepsilon_{\mathrm{osc}}}{J_{\mathrm{i}}}\left(\frac{2\omega^2 \nu_{\mathrm{eff}}}{\omega^2 + \nu_{\mathrm{eff}}^2}\right) \tag{8}$$

where ν_{eff} is the effective collision frequency of electrons with a lattice (ions), n_{ph} is the number of photons needed for overcoming the ionization potential, and the electron quivering energy in the laser field is described as

$$\varepsilon_{\mathrm{osc}}\ (\mathrm{eV}) = 9.3\frac{I}{10^{14}\ (\mathrm{W\ cm^{-2}})}(\lambda\ (\mu\mathrm{m}))^2 \tag{9}$$

where λ is the laser wavelength.

The permittivity properties of the fused silica can be affected by the number density of the ionized electrons, which leads to the transformation of the dispersion relationship of the excited SPPs. The ripples with different periods can be formed as a result of the dynamics of the phase-matching restructuring. In section 3, we will investigate the ionization fraction distribution (defined as the ratio of the densities of the ionized electrons and the valence band atoms) with respect to the pulse-to-pulse separation and the fluence. The results will be useful for analysis of the SPP dispersion wavelength transformations during the interference phase-matching restructuring, for manipulation of the ripple period.

3. Discussion and results

The two-dimensional (2D) distributions of the ionization fraction on fused silica as functions of the laser fluence and pulse separation of the double fs pulse are shown in figure 1. The increase of the fluence from (a) to (c) results in aggregation of the ionization fraction mostly within the sub-surface region of the fused silica. This indicates that the ripples are mainly formed on the ionized SPP region when the fluence exceeds the ripple formation threshold, defined as $2N_{\mathrm{c}}$ in air ambient [18].

More interestingly, it can be seen from parts (d)–(f) that the ionization fraction distribution significantly diffuses into the inner bulk of fused silica upon increasing the pulse separation. However, the ionization fraction becomes invariant when the pulse separation falls into the picosecond time regime, which is not shown here. In terms of the above

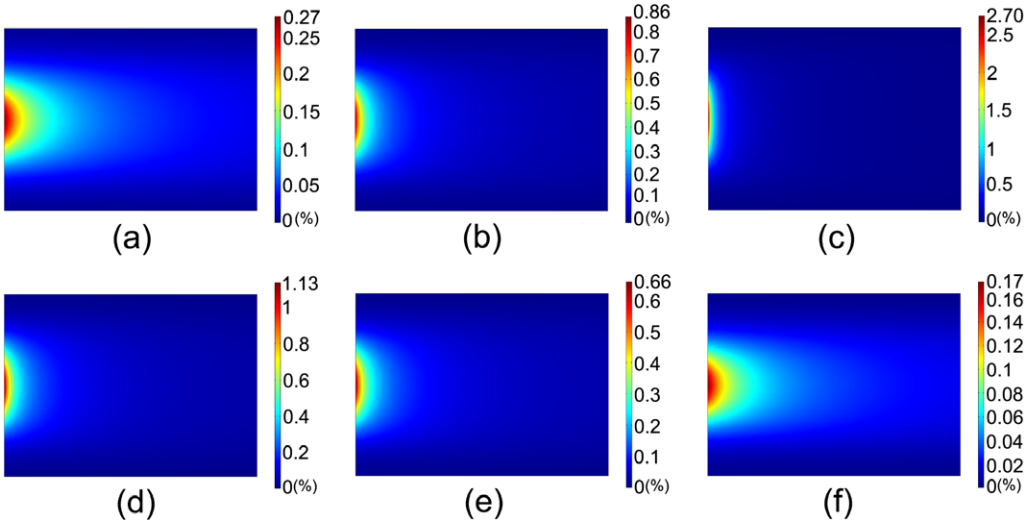

Figure 1. The two-dimensional (2D) distributions of the ionization fraction on fused silica as functions of the fluence and pulse separation. (a)–(c) show the results for different laser fluences: (a) $F = 1.6$ J cm^{-2}, (b) $F = 1.8$ J cm^{-2} and (c) $F = 2.0$ J cm^{-2}, with the pulse separation $\Delta = 150$ fs and pulse duration $t_p = 100$ fs; (d)–(f) show the results for different pulse separations: (a) $\Delta = 100$ fs, (b) $\Delta = 400$ fs and (c) $\Delta = 800$ fs, with the pulse duration $t_p = 100$ fs and laser fluence $F = 1.9$ J cm^{-2}.

investigations, the ionization fractions are all lower than the threshold for ripple formation. The ripple threshold ionization fraction is calculated as 5.29%. When the ionization fraction exceeds the threshold ionization fraction, the periodic ripples will be formed in the SPP excitation region due to the transient interference of the SPPs and the following pulse phase and Coulomb explosion.

The predicted nanoripple periods on fused silica at the center of the laser spot are shown versus the pulse separation of the train of temporally shaped double fs pulses in figure 2. According to our model, the ripple period dependences on the pulse separation of the train of shaped double fs pulses can be interpreted well in terms of the unusual ionization dynamics triggered SPP dispersion properties. When the pulse separation initially increases, the ionization fraction distribution on the fused silica decreases due to the massive diffusion of the ionization fraction into the fused silica, leading to the blue-shift of the SPP dispersion wavelength, as indicated in figure 4. The ripple period is therefore shrunk as a result of the blue-shifted SPPs in restructuring the interference phase-matching processes in the ionized region. When the pulse separation exceeds 2 ps, which accounts for the effective plasma lifetime (EPL) including the combined effects of recombination, trapping and plasma shielding [9], the variations of the pulse separation can have less effect on the ionization fraction distribution on the fused silica, as indicated in figure 1. Therefore, the SPP dispersion wavelength is frozen during the ripple patterning, which leads to a saturated ripple period due to the unaltered wavevector-matching condition, as shown in equation (1). The simulation results mostly match well with recent experimental works [9]. A data point at a pulse separation of about 2 ps is away from the calculated curve, which may arise from the instability of the laser system.

The ripple period for the central ionized region on the fused silica surface as a function of the fluence of

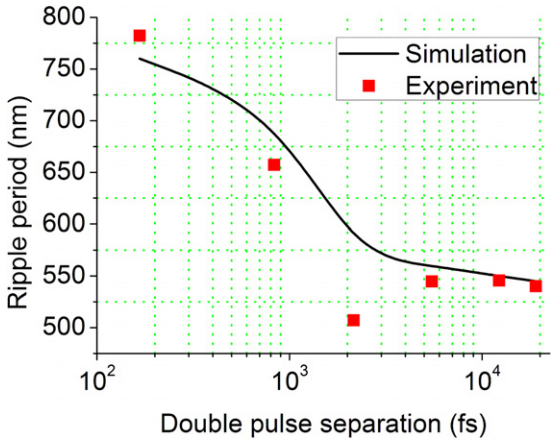

Figure 2. The predicted nanoripple periods on fused silica at the center of the laser spot versus the pulse separation of the train of temporally shaped double fs pulses (six pairs of double fs pulses are included in the train). $F = 5.3$ J cm^{-2}. The experimental results are cited from [9].

the shaped double fs pulses is shown in figure 3. The ionization fraction versus the applied fluence is also indicated. An almost linear increase in the ionization fraction with increasing laser fluence was found. The ripple period presents a rapid rise when the fluence is less than 5.0 J cm^{-2}, but tends to approach the saturation value of 730 nm when the fluence exceeds 5.0 J cm^{-2}. We can see from figure 4 that when the ionization fraction is less than the value 19%, corresponding to the excitation fluence of 5.0 J cm^{-2}, the SPP dispersion wavelength presents a rapid rise in the range of the lower ionization fraction, which indicates an active dispersion regime. However, when the SPPs drop out the active dispersion regime, the SPP wavelength cannot be affected by the ionization fraction. Considering the linear relationship between the ripple period and the SPP dispersion

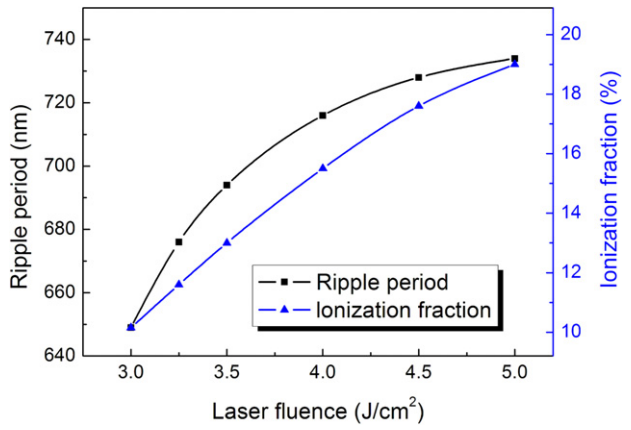

Figure 3. The ripple period at the central ionized region of the fused silica and the ionization fraction as functions of the fluence of the double fs pulses. The pulse duration $t_p = 200$ fs, the pulse separation $\Delta = 150$ fs, and the laser wavelength $\lambda = 800$ nm.

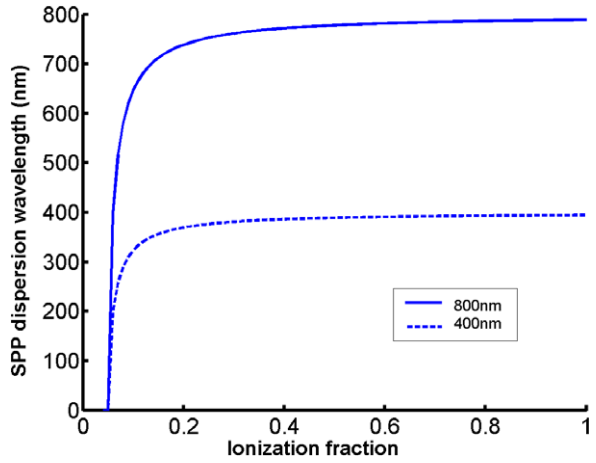

Figure 4. The SPP dispersion wavelengths for excited fused silica as functions of the ionization fraction for different incident laser wavelengths.

wavelength [18], the ripple period also presents a rapid rise when the fluence is less than 5.0 J cm^{-2}, and eventually tends to saturation. Interestingly, the SPP wavelengths approach the saturation lines almost synchronously for the light with the fundamental frequency and that with the doubled frequency. This indicates that the incident wavelength is playing a key role in regulating the ripple period, but can affect the saturation law less during the patterning of the nanoripples.

4. Conclusions

In conclusion, we have theoretically investigated the ultrafast electron dynamics manipulation for laser induced nanoripples via a train of double fs pulses. The simulations revealed that the ripple period decreases rapidly with increasing pulse separation in the sub-picosecond time regime, but approaches saturation after 2 ps. The increase of the fluence of the double fs pulse can lead to saturated augmentation of the ripple period when the fluence is larger than 5.0 J cm^{-2}. The ripple period modifications are consistently attributable to the ultrafast dynamics manipulation for the SPP dispersion wavelength through the unusual ionization via the train of shaped pulses. The present study is a key step towards determination of an ultrafast excitation mechanism for controlling laser induced periodic ripple features under irradiation with a train of shaped femtosecond laser pulses.

Acknowledgments

This work was supported by the National High Technology R&D Program of China under Grant No. 2009AA04Z305, the National Science Foundation of China under Grant No. 61176113 and the Fundamental Research Funds for the Central Universities.

References

[1] Zhao Q, Ciobanu F, Malzer S and Wang L 2007 *Appl. Phys. Lett.* **91** 121107
[2] Crouch C, Carey J, Warrender J, Aziz M, Mazur E and Génin F 2004 *Appl. Phys. Lett.* **84** 1850
[3] Chen J, Lai W, Kao Y, Yang Y and Sheu J 2012 *Opt. Express* **20** 5689
[4] Shimotsuma Y, Kazansky P, Qiu J and Hirao K 2003 *Phys. Rev. Lett.* **91** 247405
[5] Chowdhury I, Xu X and Weiner A 2005 *Appl. Phys. Lett.* **86** 151110
[6] Liebig C, Srisungsitthisunti P, Weiner A and Xu X 2010 *Appl. Phys.* A **101** 487
[7] Stoian R, Boyle M, Thoss A, Rosenfeld A, Korn G, Hertel I and Campbell E 2002 *Appl. Phys. Lett.* **80** 353
[8] Du G, Chen F, Yang Q, Si J and Hou X 2011 *Opt. Commun.* **284** 640
[9] Rohloff M, Das S, Höhm S, Grunwald R, Rosenfeld A, Krüger J and Bonse J 2011 *J. Appl. Phys.* **110** 014910
[10] Garrelie F, Colombier J, Pigeon F, Tonchev S, Faure N, Bounhalli M, Reynaud S and Rarriaux O 2011 *Opt. Express* **19** 9035
[11] Huang M, Zhao F, Cheng Y, Xu N and Xu Z 2009 *ACS Nano* **3** 4062
[12] Golosov E, Ionin A, Kolobov Yu, Kudryashov S, Ligachev A, Makarov S, Novoselov Y, Seleznev L, Sinitsyn D and Sharipov A 2011 *Phys. Rev.* B **83** 115426
[13] Arya K, Su Z and Birman J 1985 *Phys. Rev. Lett.* **54** 1559
[14] Itina T and Shcheblanov N 2010 *Appl. Phys.* A **98** 769
[15] Fauchet P and Siegman A 1982 *Appl. Phys. Lett.* **40** 824
[16] Sipe J, Young J, Preston J and van Driel H 1983 *Phys. Rev.* B **27** 1141
[17] Wu X, Jia T, Zhao F, Huang M, Xu N, Kuroda H and Xu Z 2007 *Appl. Phys.* A **86** 491
[18] Chakravarty U, Ganeev R, Naik P, Chakera J, Babu M and Gupta P 2011 *J. Appl. Phys.* **109** 084347